Impact of phosphate concentration on the metabolome of biofilms of the marine bacterium Pseudoalteromonas lipolytica

Nathan Carriot, Raphaëlle Barry-Martinet, Jean-François Briand, Annick Ortalo-Magné, Gérald Culioli

Impact of phosphate concentration on the metabolome of biofilms of the marine bacterium *Pseudoalteromonas lipolytica*

Nathan Carriot[1], Raphaëlle Barry-Martinet[1], Jean-François Briand[1], Annick Ortalo-Magné[1,*], Gérald Culioli[1,2*]

[1]*Université de Toulon, Laboratoire MAPIEM, EA 4323, La Garde, France*

[2]*Institut Méditerranéen de Biodiversité et d'Ecologie marine et continentale (IMBE), UMR CNRS-IRD-Avignon Université-Aix-Marseille Université, Avignon, France*

Corresponding authors: Annick Ortalo-Magné (annick.ortalo-magne@univ-tln.fr), Gérald Culioli (gerald.culioli@univ-avignon.fr)

Orcid ID: Nathan Carriot (0000-0001-8732-2755)
Raphaëlle Barry-Martinet (0000-0002-9147-7503)
Jean-François Briand (0000-0001-8729-2621)
Annick Ortalo-Magné (0000-0001-8899-3067)
Gérald Culioli (0000-0001-5760-6394)

Abstract

Introduction Marine biofilms are the most widely distributed mode of life on Earth and drive biogeochemical cycling processes of most elements. Phosphorus (P) is essential for many biological processes such as energy transfer mechanisms, biological information storage and membrane integrity.

Objectives Our aim was to analyze the effect of a gradient of ecologically relevant phosphate concentrations on the biofilm-forming capacity and the metabolome of the marine bacterium *Pseudoalteromonas lipolytica* TC8.

Methods In addition to the evaluation of the effect of different phosphate concentration on the biomass, structure and gross biochemical composition of biofilms of *P. lipolytica* TC8, untargeted metabolomics based on liquid chromatography-mass spectrometry (LC-MS) analysis was used to determine the main metabolites impacted by P-limiting conditions. Annotation of the most discriminating and statistically robust metabolites was performed through the concomitant use of molecular networking and MS/MS fragmentation pattern interpretation.

Results At the lowest phosphate concentration, biomass, carbohydrate content and three-dimensional structures of biofilms tended to decrease. Furthermore, untargeted metabolomics allowed for the discrimination of the biofilm samples obtained at the five phosphate concentrations and the highlighting of a panel of metabolites mainly implied in such a discrimination. A large part of the metabolites of the resulting dataset were then putatively annotated. Ornithine lipids were found in increasing quantity when the phosphate concentration decreased, while the opposite trend was observed for oxidized phosphatidylethanolamines (PEs).

Conclusion This study demonstrated the suitability of LC-MS-based untargeted metabolomics for evaluating the effect of culture conditions on marine bacterial biofilms. More

precisely, these results supported the high plasticity of the membrane of *P. lipolytica* TC8, while the role of the oxidized PEs remains to be clarified.

Keywords Marine biofilms . LC-MS-based metabolomics . Phosphate depletion . Membrane remodeling . Ornithine lipids

1 Introduction

Biofilms constitute a mode of life widely distributed in marine environments. These complex communities of marine microorganisms mainly composed of bacteria (but also archaea, diatoms and fungi) can develop on most biotic and abiotic surfaces immersed in seawater (Carvalho 2018; Dang and Lovell 2016). In biofilms, microbial cells are embedded in a three-dimensional, highly hydrated matrix of self-produced extracellular polymeric substances (EPS) mainly composed of polysaccharides and proteins, even lipids and extracellular DNA have been also described as matrix constituents (Flemming 2016; Flemming et al. 2016). This matrix promotes adhesion processes on surfaces and maintains the cohesion between biofilm microorganisms. Furthermore, the biofilm matrix acts as a nutrient source by trapping nutrient elements and molecules, or by the degradation of constitutive EPS, and protects the microbial cells against a wide range of environmental stresses (Flemming and Wingender 2010). Thus, the biosynthesis by biofilm cells of biopolymers and metabolites reflects the adaptive capacities of microbial communities to environmental constraints.

Marine biofilms play crucial roles in marine ecosystems through their implication in biogeochemical cycles and trophic interactions (Anderson 2016). In such living structures, the phenotypic plasticity of some bacteria results in their quick responses to the highly fluctuating marine conditions (Stocker 2012). Similar to hydrodynamic conditions or the nature of the colonized substrate, the availability of nutrients in the marine environment is one of the most important factors influencing biofilm development, as well as its species and biochemical compositions (Allan et al. 2002; Lawes et al. 2016). More particularly, phosphorus (P) is an essential micronutrient for living organisms (Karl 2014). Whether in its organic or inorganic forms, P is present in most compartments of both terrestrial and marine ecosystems, such as water, soil or sediment. Phosphate is generally present in low amounts in oceans with concentrations ranging typically from nanomolar values in surface waters increasing with depth

to micromolar values (Paytan and McLaughlin, 2007). In living microorganisms, P is considered an essential element, as it is involved through adenosine phosphates or NADPH in a wide range of energy-requiring reactions. P also enters, in the form of a phosphate group, the composition of DNA and RNA molecules, phosphoproteins, polyphosphates, as well as phospholipids which are key components of cell membranes (Violaki et al. 2018). The main sinks of organic P are nucleic acids, phosphoproteins and phospholipids whose biosynthesis creates a demand for this nutrient. While nucleic acids and phosphoproteins cannot be synthesized without P, the strategy of polar lipids remodeling is widespread among phytoplankton and diverse marine heterotrophic bacteria (Carini et al. 2015; Sebastián et al. 2016; Van Mooy et al. 2009). Under P deficiency, these organisms have developed strategies to maintain the membrane integrity by replacing amphiphilic membrane phospholipids with non-P lipids whose variable polar head groups contain sulfur (sulfolipids), mono- or disaccharides (glycolipids), betaines (betaine lipids) or amino acids (aminolipids) (Diercks et al. 2015; Geiger et al. 2010). Therefore, while it is well accepted that the biochemical composition of bacterial membranes varies from one microorganism to another, such a variability has been also demonstrated within a same species depending on environmental factors, and more particularly P limitations (Sohlenkamp and Geiger 2016).

The Mediterranean Sea is overall one of the most oligotrophic marine environments in the world, with the exception of specific coastal locations with anthropogenic inputs, where mineral nutrients, and particularly P, are present in limited quantity (Wambeke et al. 2002). P concentrations are so low in such locations that this nutrient is often considered to be the major limiting element for bacterial growth in Mediterranean marine environments (Dyhrman et al. 2007; Pinhassi et al. 2006). Among different groups from the heterotrophic bacterial community of the eastern Mediterranean Sea tested for their response to P availability, previous results have shown contrasting levels of bacterial metabolic activity (*i.e.* assimilation of leucine determined

using micro-autoradiography combined with fluorescence *in situ* hybridization), with γ-proteobacteria activity being the most stimulated in P-rich conditions (Sebastián and Gasol 2013).

For the present study, the impact of P starvation was evaluated on a marine bacterial strain belonging to the *Pseudoalteromonas* genus (γ-proteobacteria class), which is commonly represented in marine environments. Moreover, bacteria species of the genus *Pseudoalteromonas* show adaptative advantages such as the ability to exude a large number of EPS (Poli et al. 2010) and to produce a wide range of bioactive chemicals (Offret et al. 2016). The strain selected for this study, *Pseudoalteromonas lipolytica* TC8, had previously been isolated from a natural biofilm formed on a silicon coupon immersed in the bay of Toulon, France (NW Mediterranean Sea) (Brian-Jaisson et al. 2014; Camps et al. 2011). *P. lipolytica* TC8 was chosen as a suitable candidate to study the impact of P starvation on marine biofilms formed *in vitro* due to its capacity to easily grow *in vitro* in biofilm mode. Moreover, previous investigations of *P. lipolytica* TC8 biochemical production have shown the ability of this bacterial strain to biosynthesize, in addition to phospholipids, non-P lipids such as aminolipids (Favre et al. 2017, 2018, 2019).

In this context, LC-MS-based untargeted metabolomics appears as a well-suited approach to assess the effect of an environmental factor on organisms and has already proven effective for the analysis of marine biofilms (Bauermeister et al. 2019; Favre et al. 2017, 2018, 2019). Over the past decades, technological progress in chromatography and mass spectrometry has revolutionized this field of metabolomics. For example, these advances allow for the comparison of the metabolism of living organisms under different conditions and, more precisely, for the identification of metabolites which were differently expressed (Chang et al. 2021). For this last point, statistical analyses combined with the powerful molecular networking

approach (Aron et al. 2020; Nothias et al. 2018; Wang et al. 2016) help in the annotation of specific chemomarkers.

The annotation of metabolites of interest is always a delicate step in LC-MS-based metabolomics, as many of the LC-MS signals are inherent to samples collection and treatment (e.g. contaminants, degradation products), or related to a single molecule (e.g. adducts, fragments). At the beginning of the annotation process, a *m/z* feature can be defined by: (i) its retention time, (ii) its accurate mass and then its molecular formula, and eventually (iii) its MS/MS fragmentation pattern (fragment ions, neutral losses). If a chemical standard is available, the comparison of these three criteria (or at least of the first two) with those of the unknown feature leads easily to a robust and efficient annotation. If this is not the case, the search for accurate mass/molecular formula with or without MS/MS data in the literature regarding the studied organism and/or in specialized databases (e.g. PubChem, HMDB, MetLin, Lipidmaps) can also allow for the annotation of a specific *m/z* feature, however with a lower level of confidence (Chaleckis et al. 2019). More recently, a bioinformatic tool known as molecular networking (MN) has been developed and allows, on the theoretical basis that similar chemical structures tend to give closely-related MS/MS data, for the facilitation of the annotation step of the LC-MS-based metabolomics workflow (Watrous et al. 2012). Such a MN provides a map of the chemical space of a set of samples where nodes can be annotated not only by spectral comparison with spectral libraries and commercial/in-house compound databases (Fox Ramos et al. 2019), but also by comparing their MS/MS data with those of other nodes found in a common cluster (e.g. Carriot et al. 2021).

In this study, the aim was to investigate the impact of P starvation on the metabolism of a model biofilm-forming marine bacterium, *P. lipolytica* TC8, by mimicking relevant environmental conditions. For that purpose, five minimal culture media, in which phosphate concentration was modified in an ecologically-relevant manner to correspond to different ocean and sea conditions

over the world, were used to evaluate the resulting changes on the biofilm-forming capacity and the metabolome of *P. lipolytica* TC8. Moreover, the metabolomics workflow used in this study focused on the annotation of key discriminating and statistically robust metabolites depending on the P concentrations.

2 Materials and methods

2.1 Preparation of bacterial cultures

Pseudoalteromonas lipolytica TC8 is a γ-proteobacterium isolated from an artificial substratum immersed in the bay of Toulon (NW Mediterranean Sea, France; 43°06′23″N, 5°57′17″E) (Brian-Jaisson et al. 2014; Camps et al. 2011). Cells of *P. lipolytica* TC8, stored at -80 °C, were placed in a sterile flask containing 30 mL of Väätänen nine salt solution (VNSS) (Mårdén et al. 1985). Precultures were made in triplicate and the flasks were placed for 48 h at 20 °C in an incubator shaker (120 rpm). Bacterial precultures were subsequently diluted in VNSS in three Erlenmeyer flasks to reach an optical density at 600 nm (OD_{600}) of 0.1. The resulting precultures were incubated at 20 °C with stirring at 120 rpm. The optical density was monitored every hour until the end of the exponential phase (OD_{600} 0.6) with a spectrophotometer (Genesys 20 spectrophotometer; Thermo Fisher Scientific, Waltham, MA, USA). Medium blanks were also prepared in parallel with only VNSS. Once the precultures reached an OD_{600} equal to 0.6, 30 mL of the bacterial cultures were placed in 50 mL Falcon tubes in triplicate for each culture medium. The tubes were centrifugated (Z 200 A; Hermle LaborTechnik GmbH, NJ, USA) at 6000 rpm for 10 min at room temperature and the supernatants were removed. The resulting pellets were suspended in 15 mL of nine salt solution (NSS) (Dahlbäck et al. 1981) and then vortexed. The tubes were centrifuged at 4000 rpm for 15 min at room temperature. The supernatants were removed and the pellets were diluted in marine minimal medium (MMM) (Ostling et al. 1991) with different phosphate concentrations (Table 1 and see Part 3.1)

chosen to mimic different realistic environmental conditions. The optical densities were adjusted (OD_{600} 0.5) at that time, corresponding to a bacterial density of about 5×10^6 CFU/mL. For the following experiments, several types of culture containers were used. However, they are all made of the same material (polystyrene) and, in all experiments, they were inoculated with the same precultures at an identical optical density.

2.2 Characterization of the biofilms of *P. lipolytica* TC8

2.2.1 Biofilm quantification

Biofilm forming ability and monitoring of the evolution of bacterial biofilms according to phosphate concentration were carried out through crystal violet (CV) staining. CV allows the quantification of biofilm biomass, exopolymeric matrix and bacterial (living and dead) cells being stained (Kragh et al. 2019). More precisely, 5 mL of a bacterial preculture were placed in each well of a 6-well polystyrene plate (Greiner Bio One, Frickenhausen, Germany). Biofilms and medium blanks were made in triplicate. The plates were then incubated at 20 °C. After 24 h, the medium was removed, and the wells were rinsed three times with 6 mL of NSS. The plates were subsequently dried in an oven (50 °C, 30 min) and 5 mL of a CV solution (0.01 %) were deposited in each well. After 10 min, the plates were rinsed three times with 5 mL of Milli-Q water (Waters-Millipore, Milford, MA, USA), dried at room temperature for 10 min, and 5 mL of 95 % ethanol (VWR, Fontenay-sous-Bois, France) were added directly in the wells. An incubation time of 10 min at 20 °C under shaking (120 rpm) was performed. Finally, 200 μL of the solution of each well were transferred to a 96-well plate (Greiner Bio-One) and analyzed with a microplate reader (Infinite® M200 pro; TECAN, Switzerland) at 595 nm (Fig. 1A).

2.2.2 Biofilm viability and cellular organization

The monitoring of cell evolution was performed using the “live/dead” kit (Bacterial Viability Kit; Thermo Fisher Scientific, Eugene, OR, USA) which consists of two fluorescent markers: SYTO® 9 (labelling all the bacterial cells) and propidium iodide (PI) (labelling only dead cells). The staining was done directly in 96-well black polystyrene microplates with a clear bottom (Corning Incorporated, NY, USA). Bacterial samples and medium blanks were tested in triplicate. 200 μL of preculture were placed in each well and incubated at 20 °C. After 24 h, the wells were rinsed three times with 200 μL of a NaCl solution (36 g/L). 0.3 μL of the staining solution (PI at 20 mM/SYTO® 9 at 3.34 mM; 1/1, v/v) were then introduced in each well. Incubation was done at room temperature in the dark for 15 min. Each well was rinsed three times (NaCl at 36 g/L, 200 μL/well) in order to remove the excess of fluorescent markers. 200 μL of NaCl (36 g/L) were put in the wells which were then analyzed by a microplate reader. The absorbance wavelengths used were those of PI (538/617 nm) and SYTO® 9 (470/515 nm). A confocal microscope reading (Zeiss LSM 510 meta, Göttingen, Germany) was also performed to highlight the viability and the cellular organization of the biofilms (Fig1B).

2.2.3 Gross biochemical composition

For these assays, biofilms were obtained from 200 μL of a bacterial preculture placed in each well of 96-well polystyrene plates (Greiner Bio One). These plates were then incubated at 20 °C. After 24 h, the plates were removed and rinsed with 150 μL of NSS. The protein content of the biofilm samples was quantified by the Bradford-based Uptima coo protein assay (Interchim, Montluçon, France). The carbohydrate content was determined by a colorimetric method with glucose as a standard (DuBois et al. 1956). In this method, the use of concentrated sulfuric acid allows the obtention of monosaccharides through acidic hydrolysis of biofilm samples and leads to furfural derivatives which form colored complexes with phenol (maximum absorbance wavelength at 490 nm). Each quantification experiment was performed in triplicate (Supplemental Fig. S1).

2.3 Metabolomic analysis

2.3.1 Sample preparation

The biofilm cultures were done in polystyrene Petri dishes in which 25 mL of preculture (OD_{600} 0.5) were inoculated (24 h, 20 °C) and each medium was tested in triplicate. The supernatants of the Petri dishes were removed to keep only the biofilms and to eliminate the bacterial planktonic cells. Each Petri dish was rinsed two times with 3 mL of the corresponding culture medium. The resulting solution containing the adherent biofilm was placed in a tube. For each sample, the quenching and the extraction were carried out simultaneously by adding 5 mL of ethyl acetate (analytical grade; Carlo Erba Reagents, Peypin, France) in each tube and by vortexing the mixture (Favre et al. 2017). The tubes were then placed in an ultrasonic bath (Bransonic 2150E-DTH; Danbury, CT, USA) for 30 min at a temperature of 20 °C. The upper phase containing the organic extract was placed in 8 mL vials and dried under N_2. The vials were then filled with argon and kept at -20 °C. Medium blanks (in triplicate for each culture condition) were also prepared using the same protocol, however without bacterial cells.

2.3.2 UHPLC-MS data acquisition

The bacterial dried extracts (mass values ranging from 8 to 10 mg) and the medium blanks (mass values ranging from 3 to 7 mg) were solubilized in 1 mL of LC-MS grade methanol (Fisher, Loughborough, UK). A pool sample solution was prepared taking 100 μL of each sample (biofilms and medium blanks). The resulting solution was divided into several HPLC vials that were used as quality-control samples (QCs). At the beginning of the injection sequence, two analytical blanks (methanol only) and a QC sample (×10) were injected prior to the samples. Biofilms and medium blanks were then randomly injected to avoid any possible time-dependent changes in LC−MS chromatographic fingerprints while a QC sample was

injected every five samples. Two analytical blanks (methanol only) and a QC sample were then injected at the end of the sequence run.

Sample were analyzed by UHPLC-ESI-QToF-MS in positive mode. The UHPLC−MS instrumentation consisted of a Dionex Ultimate 3000 Rapid Separation (Thermo Fisher Scientific, Sunnyvale, CA, USA) chromatographic system equipped with a RS pump, a temperature-controlled autosampler, a thermostated column compartment and an UV-Vis diode array detector. This system was coupled via an ESI interface to a QToF Impact II mass spectrometer (Bruker Daltonics, Champs-sur-Marne, France). The separations were carried out on a reverse phase column (150 × 2.1 mm, 1.7 μm, Kinetex Phenyl-Hexyl; Phenomenex, Le Pecq, France) equipped with a pre-column (SecurityGuard cartridge; Phenomenex). The column oven temperature was maintained at 40 °C and the flow rate was set at 0.5 mL/min. The autosampler temperature was set at 4 °C and the injection volume was 5 μL. Mobile phases were: (A) water and (B) acetonitrile (LC-MS grade; Carlo Erba Reagents) containing each 0.1 % (v/v) of formic acid (Ultra grade Fluka; Sigma-Aldrich, St Quentin-Fallavier, France). The elution gradient started at 5 % B and was maintained for 2 min, then increased to 100 % B (linear ramp) in 8 min and was maintained for 4 min. The composition of the mobile phase was restored at 5 % B (linear ramp) over 0.01 min and was maintained for 1.99 min, for a total run time of 16 min.

The capillary voltage of the MS spectrometer was set at 4500 V (positive mode), and the nebulizing parameters were set as follows: nebulizing gas (N_2) pressure at 0.4 bar, drying gas (N_2) flow at 4 L/min, and drying temperature at 180 °C. Mass spectra were recorded from *m/z* 50 to 1200 at a mass resolving power of 25,000 full width at half-maximum (FWHM, *m/z* = 200) and a frequency of 2 Hz. Tandem mass spectrometry analyses were performed thanks to a collision induced dissociation (CID), fragmenting the two most intense precursor ions by scan, with a collision energy selected on the basis of the ion mass (ramp from 15 to

45 eV). A solution of formate/acetate forming clusters was automatically injected before each sample for internal mass calibration, and the mass spectrometer was calibrated with the same solution at the beginning of the injection sequence.

2.3.3 Data processing and statistical analysis

LC-MS raw data were respectively converted into ".netCDF" files using DataAnalysis (version 4.3; Bruker Daltonics) and processed with MZmine-2.51 (Pluskal et al. 2010). The data matrix was submitted to three filtering steps using an in-house script on R. Each step of the script consisted of removing successively experimental and analytical bias according to signal/noise ratio (using blanks; minimal S/N ratio: 6), coefficient of variation (using QCs; minimal CV: 20 %), and coefficient of correlation (using biofilm samples; minimal CC: 80 %). For multivariate analyses, the resulting data matrix was $\log_{10}$-transformed, mean-centered and analyzed using MetaboAnalyst 5.0 online webtool (https://www.metaboanalyst.ca/ ; Chong et al. 2019). Data were analyzed using principal component analysis (PCA), followed by partial least squares discriminant analysis (PLS-DA) to reveal differences between biofilms of *P. lipolytica* TC8 grown with various phosphate concentrations. The VIPs (variable importance in the projection) representing the most discriminating *m/z* features between the different culture conditions were classified according to their VIP score (the most discriminating metabolite having the highest VIP score) (Table 2 and Supplemental Table S1).

2.3.4 Feature annotation via molecular networking

Raw UPLC-MS/MS data were converted into ".mzXML" files using DataAnalysis. For each culture condition, the MS/MS data of one biofilm sample and one medium blank were used to build a molecular network (MN). The Global Natural Products Social Molecular Networking online workflow (GNPS web platform; http://gnps.ucsd.edu) was used to create a MN of related compounds based on the similarity of their tandem MS fragmentation patterns (Wang et al.

2016). The principle of MN was based on the fact that molecules with similar chemical structures share similar MS/MS fragmentation pathways leading to common fragment ions and neutral losses. From MS/MS spectra, the creation of a MN allowed for: (i) the identification of clusters of related compounds, (ii) the detection of a set of structural analogues of a reference molecule, and (iii) the comparison of the metabolic production of different samples. The parameters used are: precursor ion mass tolerance (Da): 0.02, fragment ion mass tolerance (Da): 0.02, minimum cosine score: 0.70, minimum matched fragment ions: 6 and network TopK: 10. Data from GNPS platform were imported into Cytoscape (version 3.7.0), using nodes to represent each spectrum and edges to represent a similarity of MS/MS fragmentation between two connected nodes (Fig. 3).

The MN thus created was used to annotate metabolites of *P. lipolytica* TC8, and more specifically the VIPs. Various methods were used to annotate a metabolite: (i) during the computational process for generating the network, GNPS platform performed a fragment similarity search of each *m/z* feature in several public databases (e.g. MassBank, HMDB) and the results of this search were directly available into the Cytoscape network, (ii) MS and MS/MS data were compared with other databanks, such as PubChem (https://pubchem.ncbi.nlm.nih.gov), ChemSpider (www.chemspider.com), Lipidmaps (http://www.lipidmaps.org), CEU mass mediator (http://ceumass.eps.uspceu.es/) and Metlin (https://metlin.scripps.edu) (Tautenhahn et al. 2012), (iii) MS and MS/MS data as well as retention times were compared with those of molecules of our in-house database, and (iv) MS data and MS/MS fragmentation patterns of nodes belonging to a same cluster of the MN were manually interpreted using their similarity and the related bibliographic data.

3 Results and discussion

The general monitoring of biofilm formation was carried out through staining with CV, confocal laser scanning microscopy, and gross biochemical characterization, while untargeted LC-MS metabolomics coupled to molecular networking allowed for observation of main changes at the metabolome level.

3.1 Selection of ecologically relevant phosphate concentrations for the culture of biofilms of *P. lipolytica* TC8

The aim of this study was to evaluate the effect of a gradient of relevant environmental P concentrations on biofilms of *P. lipolytica* TC8 (Table 1). The lowest concentration chosen corresponded to the phosphate concentration experienced by this bacterial strain in the environment from which it has been isolated (i.e. bay of Toulon, NW Mediterranean Sea). This geographical area is typically defined as nutrient limited, mostly due to a lack of phosphate (Lazzari et al. 2016), but its coastal bay waters contain higher levels of phosphate (10^{-4} mM). The second concentration (10^{-3} mM) corresponded to maximum phosphate concentrations observed in coastal locations from the NE Atlantic Ocean (Michaels et al. 1996)) and mean phosphate concentrations observed in the Baltic Sea (Frumin 2013). The third concentration (10^{-2} mM) tended to mimic phosphate levels reached in estuarine ecosystems with higher river discharges (Lochet and Leveau 1990). The last concentration corresponded to the concentration of the marine minimal medium (1.32 mM), often used to isolate and grow marine bacteria in "realistic" conditions (Patrauchan et al. 2005). Finally, an intermediate concentration of 10^{-1} mM between 10^{-2} and 1.32 mM was selected in order to avoid big gaps between phosphate concentration values along the selected gradient.

3.2 Impact of phosphate concentration on the amount and the structure of biofilms of *P. lipolytica* TC8

Growing bacteria in minimum and well-defined culture media has several advantages, such as promoting biofilm formation (due to the limited availability of certain nutrients) and allowing for the observation of the specific effects of some nutrients (e.g. phosphate in this study) on the biofilm growth and properties. In addition, the use of these carbon-limited culture media tends to avoid interactions between nutrients and organic matter that could drastically alter nutrient bioavailability. Through a simple crystal violet (CV) staining assay, the influence of medium composition on the amount of biofilm formed can be investigated (Haney et al. 2018). Such a monitoring is frequently used as it allows for the evaluation of the total biofilm biomass, including the microbial cells and the surrounding exopolymeric matrix (Barraud et al. 2014).

Regarding the biofilm cultures of *P. lipolytica* TC8, a decrease in their amount was observed in dependency with the decrease of phosphate concentration (Fig.1A). With phosphate being the only modified nutrient, a direct correlation between the decrease in the P content of the culture medium and the biomass of biofilms formed was shown. More precisely, significant shifts of the quantity of biofilm were observed between the three following groups of samples: i) $1.32/10^{-1}$ mM, ii) 10^{-2} and 10^{-3} mM, and iii) 10^{-4} mM. These results echoed previous works which have also observed a decrease in the biofilm formation under P-limiting conditions (Ghosh et al. 2019; Lehtola et al. 2002; Rinaudi et al. 2006), even if the impact of phosphate starvation on cultured marine bacterial biofilms has never been studied to date.

Confocal imaging was used to quantify living/dead bacterial cells, as well as to examine the structure of biofilms of *P. lipolytica* TC8 grown under various phosphate concentrations. No differences were observed in the ratio between living and dead cells in the different culture media (data not shown). The reduction of the biofilm amounts observed by CV staining did not only come from a cell mortality induced by P starvation, but also from a reduction of the living biomass. Regardless of the culture conditions, biofilms formed by *P. lipolytica* TC8 always displayed a highly compact layer covering the entire surface. Differences, however, can be

noted in the biofilm structure (Fig. 1B). While CLSM images revealed a carpet-like appearance of the biofilm formed at the lowest phosphate concentration (10^{-4} mM), three dimensional clusters were observed at at a phosphate concentration of 10^{-3} mM. Given that an established biofilm is structured by microbial cells and EPS, the differences in the defined architecture might be due to growth rates and EPS production. Among EPS, polysaccharides participate to the structuration of biofilms by providing aggregative properties (Karygianni et al. 2020) . Here, an increased secretion of such exopolymers might be correlated with the P content of the culture medium and would be responsible of clusters formation. This hypothesis was supported by results of protein and carbohydrate measurements by colorimetric methods which revealed a significant decrease (~40 %) of carbohydrates when the P concentration goes from 1.32 mM to 10^{-4} mM while no statistically significant variations (HSD Tukey's test) were observed for the protein content along the selected gradient (Supplemental Fig. S1).

These results revealed that the quantity and the structure of biofilms of *P. lipolytica* TC8 were impacted by P starvation at the lowest phosphate concentration used in this study (10^{-4} mM).

3.3 Discrimination of biofilms of *P. lipolytica* TC8 depending on the phosphate concentration by LC-MS-based metabolomics

The untargeted LC-(+)-ESI-MS metabolomics approach designed for the analysis of biofilms of *P. lipolytica* TC8 cultured with different phosphate concentrations produced a first dataset with 728 *m/z* features. Three drastic filtering steps were applied in order to facilitate the detection and the selection of relevant ions, corresponding to the most abundant and statistically robust metabolites, and to focus the annotation effort on these specific metabolites. At the end of this treatment, only 62 *m/z* features were kept in the final data matrix (Supplemental Table S1). A first PCA analysis including blanks and QCs was implemented (Supplemental Fig. S2). First, a clear discrimination between blanks and the other samples was observed on the corresponding PCA score plot. Moreover, QCs were centered near the origin of the PCA score

plot and were sparsely scattered, relative to the observed dispersion of biofilm samples, which is in accordance with high quality data (Broadhurst et al. 2018).

When blank samples were removed from the PCA analysis and only biofilms were considered and plotted (Fig. 2A), the resulting PCA score plot showed a clear distinction between the biofilm samples according to the phosphate concentration used for each bacterial culture. Thus, these samples were discriminated along the first component, which accounted for 32.6 % of the total variance. In accordance with the effect of the lowest phosphate conditions (10^{-4} mM) on the amount and the structure of biofilms of *P. lipolytica* TC8, the samples obtained at this phosphate concentration showed a more marked difference from all other samples along the first component of the PCA.

In order to find chemomarkers linked with the P starvation, a PLS-DA five-class model was built (one class for each phosphate concentration). The corresponding PLS-DA score plot showed a similar trend to the one observed for the PCA score plot (Fig. 2B). The different biofilm samples were distinguished due to the first component (32.3 % of the total variance) from the richest (1.32 mM) phosphate-containing culture medium to the lowest (10^{-4} mM). The second component (10.1 % of the total variance) accentuated the difference between biofilms obtained with a phosphate concentration of 10^{-3} mM and those from other culture conditions. The overall quality of the model was evaluated as good through a 10-fold internal cross-validation giving R^2, Q^2 and Q^2/R^2 values greater than 0.5 ($R^2_{1\ comp.} = 0.86$, $Q^2_{1\ comp.} = 0.69$ and $Q^2_{1\ comp.}/R^2_{1\ comp.} = 0.80$) while a permutation test ($n = 100$, $p = 0.01$) allowed for its validation (Triba et al. 2015).

So, the fluctuations of the metabolome of biofilms of *P. lipolytica* TC8 through the progressive variation of phosphate concentration in the culture medium indicated a progressive and correlated biosynthetic response of bacterial cells.

3.4 Annotation of discriminant metabolites

The next step of this study was to annotate the metabolites which were the most differentially expressed by biofilms of *P. lipolytica* TC8 according to the five different culture conditions. Through the predictive PLS-DA five-model, the most discriminant *m/z* features were determined among the whole dataset using their VIP score (Table 2 and Supplemental Table S1).

From the LC-MS/MS data obtained with the biofilm samples of *P. lipolytica* TC8, a molecular network (MN) was built (Fig. 3). It was constituted by 109 nodes, most gathered in seven main clusters (labelled from A to I), from which 36 were also found in the filtered MS data matrix used for the building of the five-class PLS-DA model (58 % of the metabolites of the matrix appeared in the MN). The differences between the number of nodes detected in the MN and the number of *m/z* features of the filtered data matrix were due to: (i) the data dependent acquisition parameters used here which did not allow for the weaker ions in a first stage of tandem MS to be analyzed in MS/MS, and (ii) the filtering steps used for the MS data matrix (but not for the MS/MS data from which the MN was built).

When focusing on the ten main VIPs (Table 2) of the five-class PLS-DA model, seven of them were detected in the MN. VIPs n°1, 2, and 4 were found in cluster B, together with two other nodes (Fig. 3). The MS/MS fragmentation pattern of these five *m/z* features has already been observed in previous studies of this same bacterial strain (Favre et al. 2017, 2018, 2019). These compounds all showed an intense diagnostic fragment ion at *m/z* 115.09 ($C_5H_{11}N_2O_2$), as well as other ions at *m/z* 133 ($C_5H_{13}N_2O_2$) and 70 (C_4H_8N) (Supplemental Fig. S3), which are characteristic of amino-acid lipids known as ornithine lipids (OLs) (Moore et al. 2016). The characteristic MS/MS fragmentation of OLs included the sequential loss of (i) H_2O from the ornithine part, (ii) the fatty acid chain esterified to the hydroxyl group of the ornithine-linked fatty acid, and (iii) the amide-linked fatty acid (Zhang et al. 2009). On the basis of this MS/MS fragmentation pattern, VIPs n°1, 2 and 4 were annotated as OL (18:1/18:1), OL (16:0, 16:0)

and OL (18:1/16:0), respectively. In the same way, the two other nodes of cluster B were annotated as *lyso*-OL (18:1) and *lyso*-OL (16:0). For VIP n°3, a specific tandem MS/MS run specifically targeted on the corresponding ion allowed for an interpretable MS/MS spectrum and the annotation of this VIP as OL (14:0, 18:0).

VIP n°5 was detected in cluster C and revealed a molecular formula ($C_{19}H_{36}O_4$) and a MS/MS fragmentation pattern in accordance with those of a monoacylglycerol bearing a C16:1 fatty acyl chain (Fig.3, Table 2 and Supplemental Fig. S3) (Gao et al. 2016) . More precisely, from the protonated molecule (*m/z* 329.2693, $[C_{19}H_{37}O_4]^+$), the observed fragment ions on the MS/MS spectrum were assigned to the loss of: (i) H_2O through the ion observed at *m/z* 311.2580 $[C_{19}H_{35}O_3]^+$ ($[M - H_2O + H]^+$), (ii) the glycerol part on the basis of the acylium ion at *m/z* 237.2216 $[C_{16}H_{29}O]^+$ and the corresponding dehydrated ion at *m/z* 219.2111 $[C_{16}H_{27}]^+$, and (iii) the acyl chain through the ion at *m/z* 75.0442 $[C_3H_7O_2]^+$ ($[M - RCOOH + H]^+$). The same detailed analysis of MS/MS data of the other nodes of this cluster allowed for the annotation of another monoacylglycerol derivative and three fatty acids (Fig. 3).

VIPs n° 6 and 7 were included in the largest cluster of the MN (cluster A, Fig. 3). A large part of the nodes constituting this cluster were characterized by a MS/MS spectrum showing the most intense fragment ion obtained following a neutral loss of *m/z* 141.02 ($C_2H_8NO_4P$) from the precursor ion (Supplemental Fig. S3). Such a fragmentation pattern is typical of phosphatidylethanolamines (PEs) and corresponds to the loss of the phosphoethanolamine moiety (Godzien et al. 2015; Suárez-García et al. 2017). Thus, VIP n°6 (*m/z* 624.3879, $[C_{30}H_{59}NO_{10}P]^+$) was putatively annotated as the oxidized PE (16:0/9:0, O2) using fragment ions at *m/z* 313.2732 $[C_{19}H_{37}O_3]^+$ ($[M - C_2H_8NO_4 - C_{9:0(2O)} + H]^+$) and 245.1381 $[C_{12}H_{21}O_5]^+$ ($[M - C_2H_8NO_4 – C_{16:0} + H]^+$) for the characterization of the fatty acid groups (Table 2). Using the same procedure, the VIP n°7 was annotated as the oxidized PE (16:0/9:1; O), while 12 nodes of the same cluster were annotated as PEs and 10 others as *lyso*-PEs. Moreover, the six

remaining nodes observed in cluster A were annotated as phosphatidylglycerol lipids (PGs) on the basis of a neutral loss of *m/z* 172.01 from the precursor ion, giving intense fragment ions observed on their MS/MS data (Murphy and Axelsen 2011). Three additional *lyso*-PEs were also detected in the MN and constituted cluster I. The fact that these three nodes were not included into the cluster A can be explain by the occurrence of highly unsaturated acyl chains in their chemical structure, which should give specific MS/MS fragment ions. As for VIP n°3, a specific LC-MS/MS run allowed for the fragmentation of the ion corresponding to VIP n°8 and the annotation of this metabolite as the oxidized PE (16:1/9:1; O).

VIP n°10 was observed in cluster G (Fig. 3) and, as with the two other nodes of this cluster, showed a molecular formula and a MS/MS fragmentation pattern in accordance with those of ceramide lipids (Table 2 and Supplemental Fig. S3) (Hsu 2016).

Other compounds, such as dipeptides or phenylalanine, were also annotated in the MN leading to the final annotation of 53 metabolites belonging to eight chemical families.

Thus, using MN and analysis of MS/MS fragmentation pattern, nine from the ten first VIPs and 32 from the 62 *m/z* features of the final data matrix were putatively annotated (Table 2, Supplemental Table S1 and Fig. S3).

3.5 Membrane lipid adaptation of *P. lipolytica* TC8 under phosphate-limiting conditions

Depending on the phosphate concentration, the amounts of the most representative VIPs were given as boxplots in Fig. 4. These results revealed that several OLs (VIPs n°1 to 4) and a monoacylglycerol (VIP n°5) were increasingly biosynthesized by the bacterial cells as soon as the phosphate concentration decreased in the culture medium. About 50 % of the sequenced bacteria (mainly Gram-negative bacteria) can biosynthesize OLs and these non-phosphorous glycolipids are found more abundantly in the outer part of bacterial membranes (Sohlenkamp and Geiger 2016) . In several studies, the occurrence of OLs has been demonstrated to be related

to abiotic stresses such as nutrient-limiting conditions (in most cases, phosphate-limiting conditions; e.g. Lewenza et al. 2011), osmotic stress (e.g. Lopalco et al. 2013), increased temperatures or acidic conditions (Vences-Guzmán et al. 2012). The role of these aminolipids in non-stress related phenotypes has been also addressed (See in Sohlenkamp 2019). Our findings were thus in accordance with previous studies dealing with the effect of P limitations on bacterial membranes through an increase in the production of non-phosphorous lipids (e.g. Barbosa et al. 2018; Benning et al. 1995; Geiger et al. 2010; Lewenza et al. 2011).

Consistent with these first findings, three PEs (VIPs n°6 to 8) were under-expressed when the phosphate concentration decreased. Surprisingly, these three metabolites are oxidized PEs, while all the other annotated "non-oxidized" phospholipids (i.e. PEs, *lyso*-PEs, PGs and *lyso*-PGs) of the final dataset were not differentially expressed depending on the different phosphate concentrations. These results agreed with a previous study dealing on *P. lipolytica* TC8 cultures in non-limited phosphate conditions which has highlighted that PEs were mainly produced in biofilms rather than in planktonic cultures (Favre et al. 2018). They differed from several other studies which have described an important shift in the bacterial membrane composition, leading to a decrease production of phospholipids, such as PEs, and their subsequent substitution with non-phosphorous lipids, such as OLs, under P-limiting conditions (i.e. Sandoval-Calderón et al. 2015).

The fact that only oxidized PEs were impacted by phosphate concentration was quite interesting given that oxidized phospholipids have been attracting more and more interest over the past few years, especially in the medical field (Nie et al. 2020). In the case of membranes, the occurrence of oxidized phospholipids can drastically affect their properties and their organization (Tyurina et al. 2019).

4 Conclusion

The objective of this work was to evaluate the impact of phosphate-limiting conditions on biofilms of the bacterial strain *P. lipolytica* TC8 which had already shown its ability to biosynthesize alternative non-P analogues to phospholipids (Favre et al. 2017, 2018). Despite a moderate effect of various environmentally-relevant phosphate concentrations on the biomass, the gross polymeric composition and the structure of the biofilms of *P. lipolytica* TC8 formed *in vitro*, an untargeted LC-MS-based metabolomics analysis revealed clear differences at the metabolome level. Combining drastic filtering steps and annotation through MN, this metabolomics approach focusing on a few abundant and statistically robust annotated metabolites demonstrated that phosphate concentration generated significant changes in the chemical composition of membranes with higher amounts of the non-phosphorous OLs at low phosphate concentrations. Conversely, a decrease of oxidized PEs was observed in the same culture conditions, while the biosynthesis of non-oxidized PEs remained globally unchanged. Together with and in addition to previous works (Favre et al. 2017, 2018, 2019), all results agreed with the fact that *P. lipolytica* TC8 testified to a certain plasticity of membrane lipid composition in response to phenotypic and environmental changes. From a taxonomic perspective, such results are not particularly obvious because *Pseudoalteromonas* spp, and more broadly γ-proteobacteria, are not known for their ability to produce aminolipids such as ornithine lipids (Sohlenkamp and Geiger 2016). The analysis of

In the marine environment, bacteria must be able to adapt their membranes to maintain their biological functions. As environmental conditions are multiple and changing, associating a modification of the cytoplasmic membrane with an environmental condition is complicated in marine environment. Here, the fact of studying a single fluctuation allowed us to describe the impact of phosphate deficiency on the adaptation of the membrane of a marine bacterial strain cultivated in biofilm. This mechanism might be a selective advantage for bacteria present in environments experiencing rapid and massive P concentration changes, such as those found in

estuaries (Li et al. 2017; Lochet and Leveau 1990). Previous works have shown that bacterial OLs biosynthesis could increase under various stress conditions (e.g. temperature, pH) (Vences-Guzmán et al. 2012). So, it cannot be excluded that the lipid remodelling observed in this study was a response of *P. lipolytica* TC8 common to all types of stress and this question could be an avenue for further work.

Further research should also focus on the specific roles of the oxidized PEs described here and on the full characterization of their chemical structure through targeted natural products chemistry and annotation using MN (Carriot et al. 2021). Moreover, the coupling of such a metabolomics approach with other omics and their application to natural biofilms sampled in marine environments with P-contrasted conditions might be useful to better understand the adaptative strategies developed by marine bacteria upon P deficiency.

Acknowledgements The authors would like to acknowledge Dr S. Greff (Aix-Marseille University, IMBE, France) for the acquisition of LC-MS profiles and for the helpful discussions, and J. Dechaux (Université de Toulon, MAPIEM) for her help during the culture of biofilms and their subsequent extraction and analysis. The authors are also grateful to S. Ortalo-Magné for her careful English language editing of the manuscript.

Author contributions JFB, AOM and GC conceived and designed research. NC and RBM conducted experiments. NC, AOM and GC analyzed data. NC, JFB, AOM and GC wrote the manuscript. All authors read and approved the manuscript.

Funding This work was funded by the French Ministry of Higher Education, Research and Innovation and the University of Toulon (PhD. grant of N. Carriot). LC-MS experiments were conducted on the regional metabolomics platform MALLABAR funded by the Institute of Ecology and Environment (INEE) of the French National Centre for Scientific Research (CNRS), the Total Foundation and the French Sud-PACA regional council.

Data availability The metabolomics and metadata reported in this paper are available as supplementary material (Table S1). Raw data for LC-ESI-(+)-MS/MS experiments were deposited and are publicly available on the MassIVE platform under the IDs MSV000083860.

Compliance with ethical standards

Conflict of interest The authors declare that they have no conflict of interest.

Ethical approval This article does not contain any studies with human participants or animals performed by any of the authors.

References

Allan, V. J. M., Callow, M. E., Macaskie, L. E., & Paterson-Beedle, M. (2002). Effect of nutrient limitation on biofilm formation and phosphatase activity of a *Citrobacter sp*. *Microbiology (Reading, England)*, *148*(Pt 1), 277–288. https://doi.org/10.1099/00221287-148-1-277

Anderson, O. R. (2016). Marine and estuarine natural microbial biofilms: ecological and biogeochemical dimensions. *AIMS Microbiology*, *2*(3), 304–331. https://doi.org/10.3934/microbiol.2016.3.304

Aron, A. T., Gentry, E. C., McPhail, K. L., Nothias, L.-F., Nothias-Esposito, M., Bouslimani, A., et al. (2020). Reproducible molecular networking of untargeted mass spectrometry data using GNPS. *Nature Protocols*, *15*(6), 1954–1991. https://doi.org/10.1038/s41596-020-0317-5

Barbosa, L. C., Goulart, C. L., Avellar, M. M., Bisch, P. M., & von Kruger, W. M. A. Y. 2018. (2018). Accumulation of ornithine lipids in *Vibrio cholerae* under phosphate deprivation is dependent on VC0489 (OlsF) and PhoBR system. *Microbiology*, *164*(3), 395–399. https://doi.org/10.1099/mic.0.000607

Barraud, N., Moscoso, J. A., Ghigo, J.-M., & Filloux, A. (2014). Methods for studying biofilm dispersal in *Pseudomonas aeruginosa*. In A. Filloux & J.-L. Ramos (Eds.), *Pseudomonas Methods and Protocols* (pp. 643–651). New York, NY: Springer. https://doi.org/10.1007/978-1-4939-0473-0_49

Bauermeister, A., Pereira, F., Grilo, I. R., Godinho, C. C., Paulino, M., Almeida, V., et al. (2019). Intra-clade metabolomic profiling of MAR4 *Streptomyces* from the Macaronesia Atlantic region reveals a source of anti-biofilm metabolites. *Environmental Microbiology*, *21*(3), 1099–1112. https://doi.org/10.1111/1462-2920.14529

Benning, C., Huang, Z. H., & Gage, D. A. (1995). Accumulation of a novel glycolipid and a betaine lipid in cells of *Rhodobacter sphaeroides* grown under phosphate limitation. *Archives of Biochemistry and Biophysics*, *317*(1), 103–111. https://doi.org/10.1006/abbi.1995.1141

Brian-Jaisson, F., Ortalo-Magné, A., Guentas-Dombrowsky, L., Armougom, F., Blache, Y., & Molmeret, M. (2014). Identification of bacterial strains isolated from the Mediterranean Sea exhibiting different abilities of biofilm formation. *Microbial Ecology*, *68*(1), 94–110. https://doi.org/10.1007/s00248-013-0342-9

Broadhurst, D., Goodacre, R., Reinke, S. N., Kuligowski, J., Wilson, I. D., Lewis, M. R., & Dunn, W. B. (2018). Guidelines and considerations for the use of system suitability and quality control samples in mass spectrometry assays applied in untargeted clinical metabolomic studies. *Metabolomics*, *14*(6), 72. https://doi.org/10.1007/s11306-018-1367-3

Camps, M., Briand, J.-F., Guentas-Dombrowsky, L., Culioli, G., Bazire, A., & Blache, Y. (2011). Antifouling activity of commercial biocides vs. natural and natural-derived products assessed by marine bacteria adhesion bioassay. *Marine Pollution Bulletin*, *62*(5), 1032–1040. https://doi.org/10.1016/j.marpolbul.2011.02.031

Carini, P., Van Mooy, B. A. S., Thrash, J. C., White, A., Zhao, Y., Campbell, E. O., et al. (2015). SAR11 lipid renovation in response to phosphate starvation. *Proceedings of the National Academy of Sciences*, *112*(25), 7767–7772.

Carvalho, D. (2018). Marine biofilms: A successful microbial strategy with economic implications. *Frontiers in Marine Science*, *5*:126. https://doi.org/10.3389/fmars.2018.00126

Chaleckis, R., Meister, I., Zhang, P., & Wheelock, C. E. (2019). Challenges, progress and promises of metabolite annotation for LC–MS-based metabolomics. *Current Opinion in Biotechnology*, *55*, 44–50. https://doi.org/10.1016/j.copbio.2018.07.010

Chang, H.-Y., Colby, S. M., Du, X., Gomez, J. D., Helf, M. J., Kechris, K., et al. (2021). A practical guide to metabolomics software development. *Analytical Chemistry*, *93*(4), 1912–1923. https://doi.org/10.1021/acs.analchem.0c03581

Chong, J., Wishart, D. S., & Xia, J. (2019). Using MetaboAnalyst 4.0 for comprehensive and integrative metabolomics data analysis. *Current Protocols in Bioinformatics*, *68*(1), e86. https://doi.org/10.1002/cpbi.86

Dahlbäck, B., Hermansson, M., Kjelleberg, S., & Norkrans, B. (1981). The hydrophobicity of bacteria - An important factor in their initial adhesion at the air-water inteface. *Archives of Microbiology*, *128*(3), 267–270. https://doi.org/10.1007/BF00422527

Dang, H., & Lovell, C. R. (2016). Microbial surface colonization and biofilm development in marine environments. *Microbiology and Molecular Biology Reviews*, *80*(1), 91–138. https://doi.org/10.1128/MMBR.00037-15

Diercks, H., Semeniuk, A., Gisch, N., Moll, H., Duda, K. A., & Hölzl, G. (2015). Accumulation of novel glycolipids and ornithine lipids in *Mesorhizobium loti* under phosphate deprivation. *Journal of Bacteriology*, *197*(3), 497–509. https://doi.org/10.1128/JB.02004-14

DuBois, M., Gilles, K. A., Hamilton, J. K., Rebers, P. A., & Smith F. (1956). Colorimetric method for determination of sugars and related substances. *Analytical Chemistry*, *28*(3):350–356. https://doi.org/10.1021/ac60111a017

Dyhrman, S. T., Ammerman, J. W., & Van Mooy, B. A. S. (2007). Microbes and the marine phosphorus cycle. *Oceanography*, *20*(2), 110–116. https://www.jstor.org/stable/24860049.

Favre, L., Ortalo-Magné, A., Greff, S., Pérez, T., Thomas, O. P., Martin, J.-C., & Culioli, G. (2017). Discrimination of four marine biofilm-forming bacteria by LC-MS metabolomics and influence of culture parameters. *Journal of Proteome Research*, *16*(5), 1962–1975. https://doi.org/10.1021/acs.jproteome.6b01027

Favre, L., Ortalo-Magné, A., Kerloch, L., Pichereaux, C., Misson, B., Briand, J.-F., et al. (2019). Metabolomic and proteomic changes induced by growth inhibitory concentrations of copper in the biofilm-forming marine bacterium *Pseudoalteromonas lipolytica*. *Metallomics*, *11*(11), 1887–1899. https://doi.org/10.1039/c9mt00184k

Favre, L., Ortalo-Magné, A., Pichereaux, C., Gargaros, A., Burlet-Schiltz, O., Cotelle, V., & Culioli, G. (2018). Metabolome and proteome changes between biofilm and planktonic phenotypes of the marine bacterium *Pseudoalteromonas lipolytica* TC8. *Biofouling*, *34*(2), 132–148. https://doi.org/10.1080/08927014.2017.1413551

Flemming, H.-C. (2016). EPS - Then and now. *Microorganisms*, *4*(4), 41. https://doi.org/10.3390/microorganisms4040041

Flemming, H.-C., & Wingender, J. (2010). The biofilm matrix. *Nature Reviews Microbiology*, *8*(9), 623–633. https://doi.org/10.1038/nrmicro2415

Flemming, H.-C., Wingender, J., Szewzyk, U., Steinberg, P., Rice, S. A., & Kjelleberg, S. (2016). Biofilms: an emergent form of bacterial life. *Nature Reviews Microbiology*, *14*(9), 563–575. https://doi.org/10.1038/nrmicro.2016.94

Fox Ramos, A. E., Pavesi, C., Litaudon, M., Dumontet, V., Poupon, E., Champy, P., et al. (2019). CANPA: Computer-Assisted Natural Products Anticipation. *Analytical Chemistry*, *91*(17), 11247–11252. https://doi.org/10.1021/acs.analchem.9b02216

Frumin, G. T. (2013). Total phosphorus distribution over the Baltic Sea sub-regions. *Russian Journal of General Chemistry*, *83*(13), 2647–2650. https://doi.org/10.1134/S1070363213130094

Gao, F., McDaniel, J., Chen, E. Y., Rockwell, H., Lynes, M. D., Tseng, Y.-H., et al. (2016). Monoacylglycerol analysis using MS/MS^{ALL} quadruple time of flight mass spectrometry. *Metabolites*, *6*(3), 25. https://doi.org/10.3390/metabo6030025

Geiger, O., González-Silva, N., López-Lara, I. M., & Sohlenkamp, C. (2010). Amino acid-containing membrane lipids in bacteria. *Progress in Lipid Research*, *49*(1), 46–60. https://doi.org/10.1016/j.plipres.2009.08.002

Ghosh, R., Barman, S., & Mandal, N. C. (2019). Phosphate deficiency induced biofilm formation of *Burkholderia* on insoluble phosphate granules plays a pivotal role for maximum release of soluble phosphate. *Scientific Reports*, *9*(1), 5477. https://doi.org/10.1038/s41598-019-41726-9

Godzien, J., Ciborowski, M., Martínez-Alcázar, M. P., Samczuk, P., Kretowski, A., & Barbas, C. (2015). Rapid and reliable identification of phospholipids for untargeted metabolomics with LC–ESI–QTOF–MS/MS. *Journal of Proteome Research*, *14*(8), 3204–3216. https://doi.org/10.1021/acs.jproteome.5b00169

Haney, E. F., Trimble, M. J., Cheng, J. T., Vallé, Q., & Hancock, R. E. W. (2018). Critical assessment of methods to quantify biofilm growth and evaluate antibiofilm activity of host defence peptides. *Biomolecules*, *8*(2), 29. https://doi.org/10.3390/biom8020029

Hsu, F.-F. (2016). Complete structural characterization of ceramides as $[M-H]^-$ ions by multiple-stage linear ion trap mass spectrometry. *Biochimie*, *130*, 63–75. https://doi.org/10.1016/j.biochi.2016.07.012

Karl, D. M. (2014). Microbially mediated transformations of phosphorus in the sea: New views of an old cycle. *Annual Review of Marine Science*, *6*(1), 279–337. https://doi.org/10.1146/annurev-marine-010213-135046

Karygianni, L., Ren, Z., Koo, H., & Thurnheer, T. (2020). Biofilm matrixome: Extracellular components in structured microbial communities. *Trends in Microbiology*, *28*(8), 668–681. https://doi.org/10.1016/j.tim.2020.03.016

Kragh, K. N., Alhede, M., Kvich, L., & Bjarnsholt, T. (2019). Into the well - A close look at the complex structures of a microtiter biofilm and the crystal violet assay. *Biofilm*, *1*, 100006. https://doi.org/10.1016/j.bioflm.2019.100006

Lawes, J. C., Neilan, B. A., Brown, M. V., Clark, G. F., & Johnston, E. L. (2016). Elevated nutrients change bacterial community composition and connectivity: high throughput sequencing of young marine biofilms. *Biofouling*, *32*(1), 57–69. https://doi.org/10.1080/08927014.2015.1126581

Lazzari, P., Solidoro, C., Salon, S., & Bolzon, G. (2016). Spatial variability of phosphate and nitrate in the Mediterranean Sea: A modeling approach. *Deep Sea Research Part I: Oceanographic Research Papers*, *108*, 39–52. https://doi.org/10.1016/j.dsr.2015.12.006

Lehtola, M. J., Miettinen, I. T., & Martikainen, P. J. (2002). Biofilm formation in drinking water affected by low concentrations of phosphorus. *Canadian Journal of Microbiology*, *48*(6), 494–499. https://doi.org/10.1139/w02-048

Lewenza, S., Falsafi, R., Bains, M., Rohs, P., Stupak, J., Sprott, G. D., & Hancock, R. E. W. (2011). The olsA gene mediates the synthesis of an ornithine lipid in *Pseudomonas aeruginosa* during growth under phosphate-limiting conditions, but is not involved in antimicrobial peptide susceptibility. *FEMS microbiology letters*, *320*(2), 95–102. https://doi.org/10.1111/j.1574-6968.2011.02295.x

Li, R., Xu, J., Li, X., Shi, Z., & Harrison, P. J. (2017). Spatiotemporal variability in phosphorus species in the Pearl River estuary: Influence of the river discharge. *Scientific Reports*, *7*(1), 13649. https://doi.org/10.1038/s41598-017-13924-w

Lochet, F., & Leveau, M. (1990). Transfers between a eutrophic ecosystem, the river Rhône, and an oligotrophic ecosystem, the north-western Mediterranean Sea. *Hydrobiologia*, *207*(1), 95–103. https://doi.org/10.1007/BF00041445

Lopalco, P., Angelini, R., Lobasso, S., Köcher, S., Thompson, M., Müller, V., & Corcelli, A. (2013). Adjusting membrane lipids under salt stress: the case of the moderate halophilic organism *Halobacillus halophilus*. *Environmental Microbiology*, *15*(4), 1078–1087. https://doi.org/10.1111/j.1462-2920.2012.02870.x

Mårdén, P., Tunlid, A., Malmcrona-Friberg, K., Odham, G., & Kjelleberg, S. (1985). Physiological and morphological changes during short term starvation of marine bacterial islates. *Archives of Microbiology*, *142*(4), 326–332. https://doi.org/10.1007/BF00491898

Michaels, A. F., Olson, D., Sarmiento, J. L., Ammerman, J. W., Fanning, K., Jahnke, R., et al. (1996). Inputs, losses and transformations of nitrogen and phosphorus in the pelagic North Atlantic Ocean. *Biogeochemistry*, *35*(1), 181–226. https://doi.org/10.1007/BF02179827

Moore, E. K., Hopmans, E. C., Rijpstra, W. I. C., Villanueva, L., & Damsté, J. S. S. (2016). Elucidation and identification of amino acid containing membrane lipids using liquid chromatography/high-resolution mass spectrometry. *Rapid Communications in Mass Spectrometry*, *30*(6), 739–750. https://doi.org/10.1002/rcm.7503

Murphy, R. C., & Axelsen, P. H. (2011). Mass spectrometric analysis of long-chain lipids. *Mass Spectrometry Reviews*, *30*(4), 579–599. https://doi.org/10.1002/mas.20284

Nie, J., Yang, J., Wei, Y., & Wei, X. (2020). The role of oxidized phospholipids in the development of disease. *Molecular Aspects of Medicine*, *76*, 100909. https://doi.org/10.1016/j.mam.2020.100909

Nothias, L.-F., Nothias-Esposito, M., da Silva, R., Wang, M., Protsyuk, I., Zhang, Z., et al. (2018). Bioactivity-based molecular networking for the discovery of drug leads in natural product bioassay-guided fractionation. *Journal of Natural Products*, *81*(4), 758–767. https://doi.org/10.1021/acs.jnatprod.7b00737

Offret, C., Desriac, F., Le Chevalier, P., Mounier, J., Jégou, C., & Fleury, Y. (2016). Spotlight on antimicrobial metabolites from the marine bacteria *Pseudoalteromonas*: Chemodiversity and ecological significance. *Marine Drugs*, *14*(7), 129. https://doi.org/10.3390/md14070129

Ostling, J., Goodman, A., & Kjelleberg, S. (1991). Behaviour of IncP-1 plasmids and a miniMu transposon in a marine *Vibrio sp.*: Isolation of starvation inducible lac operon fusions. *FEMS Microbiology Letters*, *86*(1), 83–93. https://doi.org/10.1111/j.1574-6968.1991.tb04797.x

Patrauchan, M. A., Sarkisova, S., Sauer, K., & Franklin, M. J. Y. (2005). Calcium influences cellular and extracellular product formation during biofilm-associated growth of a marine *Pseudoalteromonas sp. Microbiology*, *151*(9), 2885–2897. https://doi.org/10.1099/mic.0.28041-0

Paytan, A., & McLaughlin, K. (2007). The oceanic phosphorus cycle. *Chemical Reviews*, *107*(2), 563-576. https://doi.org/10.1021/cr0503613

Pinhassi, J., Gómez-Consarnau, L., Alonso-Sáez, L., Sala, M. M., Vidal, M., Pedrós-Alió, C., & Gasol, J. M. (2006). Seasonal changes in bacterioplankton nutrient limitation and their effects on bacterial community composition in the NW Mediterranean Sea. *Aquatic Microbial Ecology*, *44*(3), 241–252. https://doi.org/10.3354/ame044241

Pluskal, T., Castillo, S., Villar-Briones, A., & Orešič, M. (2010). MZmine 2: Modular framework for processing, visualizing, and analyzing mass spectrometry-based

molecular profile data. *BMC Bioinformatics*, *11*(1), 395. https://doi.org/10.1186/1471-2105-11-395

Poli, A., Anzelmo, G., & Nicolaus, B. (2010). Bacterial exopolysaccharides from extreme marine habitats: Production, characterization and biological activities. *Marine Drugs*, *8*(6), 1779–1802. https://doi.org/10.3390/md8061779

Rinaudi, L., Fujishige, N. A., Hirsch, A. M., Banchio, E., Zorreguieta, A., & Giordano, W. (2006). Effects of nutritional and environmental conditions on *Sinorhizobium meliloti* biofilm formation. *Research in Microbiology*, *157*(9), 867–875. https://doi.org/10.1016/j.resmic.2006.06.002

Sandoval-Calderón, M., Nguyen, D. D., Kapono, C. A., Herron, P., Dorrestein, P. C., & Sohlenkamp, C. (2015). Plasticity of *Streptomyces coelicolor* membrane composition under different growth conditions and during development. *Frontiers in Microbiology*, *6*:1465. https://doi.org/10.3389/fmicb.2015.01465

Sebastián, M., & Gasol, J. M. (2013). Heterogeneity in the nutrient limitation of different bacterioplankton groups in the Eastern Mediterranean Sea. *The ISME Journal*, *7*(8), 1665–1668. https://doi.org/10.1038/ismej.2013.42

Sebastián, M., Smith, A. F., González, J. M., Fredricks, H. F., Van Mooy, B., Koblížek, M., et al. (2016). Lipid remodelling is a widespread strategy in marine heterotrophic bacteria upon phosphorus deficiency. *The ISME Journal*, *10*(4), 968–978. https://doi.org/10.1038/ismej.2015.172

Sohlenkamp, C. (2019). Ornithine lipids and other amino acid-containing acyloxyacyl lipids. In O. Geiger (Ed.), *Biogenesis of Fatty Acids, Lipids and Membranes* (pp. 109–122). Cham: Springer International Publishing. https://doi.org/10.1007/978-3-319-50430-8_13

Sohlenkamp, C., & Geiger, O. (2016). Bacterial membrane lipids: diversity in structures and pathways. *FEMS Microbiology Reviews*, *40*(1), 133–159. https://doi.org/10.1093/femsre/fuv008

Stocker, R. (2012). Marine microbes see a sea of gradients. *Science*, *338*(6107), 628–633. https://doi.org/10.1126/science.1208929

Suárez-García, S., Arola, L., Pascual-Serrano, A., Arola-Arnal, A., Aragonès, G., Bladé, C., & Suárez, M. (2017). Development and validation of a UHPLC-ESI-MS/MS method for the simultaneous quantification of mammal lysophosphatidylcholines and lysophosphatidylethanolamines in serum. *Journal of Chromatography B, 1055–1056*, 86–97. https://doi.org/10.1016/j.jchromb.2017.04.028

Tautenhahn, R., Patti, G. J., Rinehart, D., & Siuzdak, G. (2012). XCMS Online: A web-based platform to process untargeted metabolomic data. *Analytical Chemistry*, *84*(11), 5035–5039. https://doi.org/10.1021/ac300698c

Triba, M. N., Le Moyec, L., Amathieu, R., Goossens, C., Bouchemal, N., Nahon, P., et al. (2015). PLS/OPLS models in metabolomics: the impact of permutation of dataset rows on the K-fold cross-validation quality parameters. *Molecular bioSystems*, *11*(1), 13–19. https://doi.org/10.1039/c4mb00414k

Tyurina, Y. Y., St Croix, C. M., Watkins, S. C., Watson, A. M., Epperly, M. W., Anthonymuthu, T. S., et al. (2019). Redox (phospho)lipidomics of signaling in inflammation and programmed cell death. *Journal of Leukocyte Biology*, *106*(1), 57–81. https://doi.org/10.1002/JLB.3MIR0119-004RR

Van Mooy, B. A. S., Fredricks, H. F., Pedler, B. E., Dyhrman, S. T., Karl, D. M., Koblížek, M., et al. (2009). Phytoplankton in the ocean use non-phosphorus lipids in response to phosphorus scarcity. *Nature*, *458*(7234), 69–72. https://doi.org/10.1038/nature07659

Van Wambeke, F., Christaki, U., Giannakourou, A., Moutin, T., & Souvemerzoglou, K. (2002). Longitudinal and vertical trends of bacterial limitation by phosphorus and carbon in the Mediterranean Sea. *Microbial Ecology*, *43*(1), 119–133. https://doi.org/10.1007/s00248-001-0038-4

Vences-Guzmán, M. Á., Geiger, O., & Sohlenkamp, C. (2012). Ornithine lipids and their structural modifications: from A to E and beyond. *FEMS microbiology letters*, *335*(1), 1–10. https://doi.org/10.1111/j.1574-6968.2012.02623.x

Violaki, K., Bourrin, F., Aubert, D., Kouvarakis, G., Delsaut, N., & Mihalopoulos, N. (2018). Organic phosphorus in atmospheric deposition over the Mediterranean Sea: An important missing piece of the phosphorus cycle. *Progress in Oceanography*, *163*, 50–58. https://doi.org/10.1016/j.pocean.2017.07.009

Wang, M., Carver, J. J., Phelan, V. V., Sanchez, L. M., Garg, N., Peng, Y., et al. (2016). Sharing and community curation of mass spectrometry data with Global Natural Products Social Molecular Networking. *Nature Biotechnology*, *34*(8), 828–837. https://doi.org/10.1038/nbt.3597

Watrous, J., Roach, P., Alexandrov, T., Heath, B. S., Yang, J. Y., Kersten, R. D., et al. (2012). Mass spectral molecular networking of living microbial colonies. *Proceedings of the National Academy of Sciences*, *109*(26), E1743–E1752. https://doi.org/10.1073/pnas.1203689109

Zhang, X., Ferguson-Miller, S. M., & Reid, G. E. (2009). Characterization of ornithine and glutamine lipids extracted from cell membranes of *Rhodobacter sphaeroides*. *Journal of the American Society for Mass Spectrometry*, *20*(2), 198–212. https://doi.org/10.1016/j.jasms.2008.08.017

Table and figure legends

Table 1. Culture media with various ecologically relevant phosphate concentrations used in this study for the growth of biofilms of *P. lipolytica* TC8.

Growth media	Phosphate concentration (mM)	References
Marine minimum medium	**1.32**	Patrauchan et al. 2005
Intermediate medium	**10^{-1}**	-
Estuarine ecosystem medium	**10^{-2}**	Lochet and Leveau 1990
Atlantic Ocean & Baltic Sea medium	**10^{-3}**	Michaels et al. 1996, Frumin 2013
Mediterranean Sea medium (Toulon)	**10^{-4}**	Lazzari et al. 2016

Table 2. List of the first ten biomarkers (VIPs) putatively annotated by LC-MS for the chemical discrimination of biofilm extracts of *P. lipolytica* TC8 according to the phosphate concentration.

VIP number	*m/z*	RT (min)	VIP score	Molecular formula[a]	Mass error (ppm)	mσ[b]	MS/MS fragment ions (relative abundance in %)	Putative annotation
1	677.5837	11.35	4.21	$C_{41}H_{76}N_2O_5$	-1.5	2.9	395.3274 $[C_{23}H_{43}N_2O_3]^+$ (88) ; 377.3168 $[C_{23}H_{41}N_2O_2]^+$ (82) ; 280.2653 $[C_{18}H_{34}NO]^+$ (1) ; 263.2373 $[C_{18}H_{31}O]^+$ (12) ; 159.0770 $[C_6H_{11}N_2O_3]^+$ (7) ; 141.0662 $[C_6H_9N_2O_2]^+$ (2) ; 133.0977 $[C_5H_{13}N_2O_2]^+$ (6) ; **115.0870 $[C_5H_{11}N_2O]^+$ (100)** ; 70.0652 $[C_4H_8N]^+$ (26)	OL (18:1/18:1)
2	625.5501	11.16	3.16	$C_{37}H_{72}N_2O_5$	1.8	8.0	369.3112 $[C_{21}H_{41}N_2O_3]^+$ (47) ; 351.3010 $[C_{21}H_{39}N_2O_2]^+$ (46) ; 254.2479 $[C_{16}H_{32}NO]^+$ (1) ; 239.2374 $[C_{16}H_{31}O]^+$ (3) ; 159.0769 $[C_6H_{11}N_2O_3]^+$ (6) ; 141.0661 $[C_6H_9N_2O_2]^+$ (5) ; 133.0975 $[C_5H_{13}N_2O_2]^+$ (5) ; **115.0868 $[C_5H_{11}N_2O]^+$ (100)** ; 70.0653 $[C_4H_8N]^+$ (23)	OL (16:0/16:0)
3	625.5519	11.77	2.92	$C_{37}H_{72}N_2O_5$	-0.9	7.9	341.2808 $[C_{19}H_{37}N_2O_3]^+$ (2) ; 323.2699 $[C_{19}H_{35}N_2O_2]^+$ (2) ; 133.0975 $[C_5H_{13}N_2O_2]^+$ (5) ; **115.0868 $[C_5H_{11}N_2O]^+$ (100)** ; 70.0653 $[C_4H_8N]^+$ (23)	OL (14:0/18:0)[c]
4	651.5677	11.25	2.81	$C_{39}H_{74}N_2O_5$	-1.0	4.4	395.3280 $[C_{23}H_{43}N_2O_3]^+$ (37) ; 377.3172 $[C_{23}H_{41}N_2O_2]^+$ (36) ; 280.2657 $[C_{18}H_{34}NO]^+$ (1) ; 237.2219 $[C_{16}H_{29}O]^+$ (6) ; 159.0768 $[C_6H_{11}N_2O_3]^+$ (6) ; 141.0661 $[C_6H_9N_2O_2]^+$ (4) ; 133.0975 $[C_5H_{13}N_2O_2]^+$ (6) ; **115.0869 $[C_5H_{11}N_2O]^+$ (100)** ; 70.0654 $[C_4H_8N]^+$ (28)	OL (18:1/16:0)
5	329.2693	10.12	1.87	$C_{19}H_{36}O_4$	-2.1	15.8	311.2580 $[C_{19}H_{35}O_3]^+$ (11); 237.2216 $[C_{16}H_{29}O]^+$ (30) ; 219.2111 $[C_{16}H_{27}]^+$ (36) ; **81.0700 $[C_6H_9]^+$ (100)** ; 75.0442 $[C_3H_7O_2]^+$ (4)	MAG (16:1)
6	624.3879	9.81	1.27	$C_{30}H_{58}NO_{10}P$	-1.2	17.8	**483.3675 $[C_{28}H_{51}O_6]^+$ (100)** ; 313.2732 $[C_{19}H_{37}O_3]^+$ (4) ; 245.1381 $[C_{12}H_{21}O_5]^+$ (5) ; 239.2370 $[C_{16}H_{31}O]^+$ (4) ; 216.0636 $[C_5H_{13}NO_6P]^+$ (1) ; 171.10200 $[C_9H_{15}O_3]^+$ (9) ; 155.0102 $[C_3H_8O_6P]^+$ (1) ; 62.0606 $[C_2H_8NO]^+$ (11)	PE (16:0/9:0;O2)
7	608.3920	10.18	1.19	$C_{30}H_{58}NO_9P$	0.2	3.5	**467.3729 $[C_{28}H_{51}O_5]^+$ (100)** ; 313.2734 $[C_{19}H_{37}O_3]^+$ (4) ; 239.2365 $[C_{16}H_{31}O]^+$ (7) ; 229.1436 $[C_{12}H_{21}O_4]^+$ (5) ; 216.0636 $[C_5H_{13}NO_6P]^+$ (1) ; 155.1064 $[C_9H_{15}O_3]^+$ (7) ; 155.0091 $[C_3H_8O_6P]^+$ (1) ; 62.0600 $[C_2H_8NO]^+$ (1)	PE (16:0/9:1;O)
8	606.3770	9.90	0.98	$C_{30}H_{56}NO_9P$	-1.9	22.6	**465.3577 $[C_{28}H_{49}O_5]^+$ (100)** ; 311.2586 $[C_{19}H_{35}O_3]^+$ (5) ; 237.2221 $[C_{16}H_{29}O]^+$ (7) ; 229.1440 $[C_{12}H_{21}O_4]^+$ (5) ; 155.1062 $[C_9H_{15}O_2]^+$ (4) ; 155.0108 $[C_3H_8O_6P]^+$ (1) ; 62.0597 $[C_2H_8NO]^+$ (1)	PE (16:1/9:1;O)[c]
9	421.2234	10.80	0.97	$C_{23}H_{32}O_7$	-3.1	34.5	Not fragmented	–
10	524.4680	12.00	0.91	$C_{32}H_{61}NO_4$	-1.3	5.7	506.4571 $[C_{32}H_{60}NO_3]^+$ (1) ; 342.3001 $[C_{20}H_{40}NO_3]^+$ (7) ; 324.2896 $[C_{20}H_{38}NO_2]^+$ (3) ; 281.2480 $[C_{18}H_{33}O_2]^+$ (4) ; **270.2424 $[C_{16}H_{32}NO_2]^+$ (100)** ; 227.2013 $[C_{14}H_{27}O_2]^+$ (3) ; 106.0865 $[C_4H_{12}NO_2]^+$ (6) ; 88.0758 $[C_4H_{10}NO]^+$ (9)	Cer (32:2;O3)

[a] All these metabolites were observed as protonated molecules $[M+H]^+$. [b] Constructor statistical match factor (comparison of theoretical and experimental isotopic patterns). [c] Ion fragmented by targeted MS/MS analysis.

Figure 1. Effect of phosphate concentrations on biofilms of *P. lipolytica* TC8 in terms of biomass (crystal violet staining) (**1A**) and structure (CLSM images of living/dead stained cells) (**1B**).

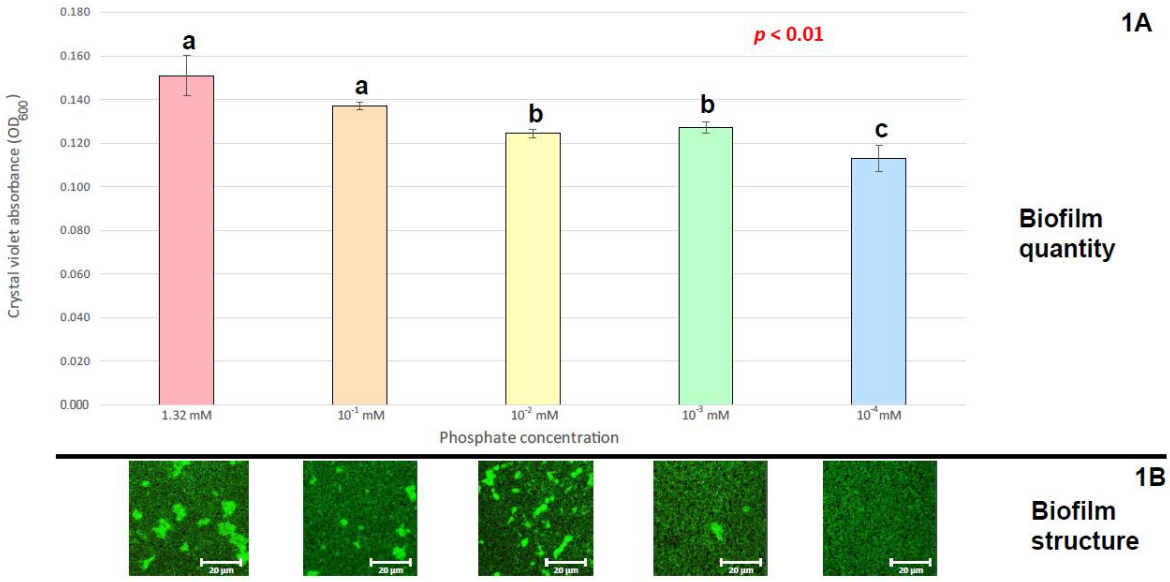

Figure 2. PCA (**2A**) and PLS-DA (**2B**) score plots obtained from (+)-ESI-LC-MS profiles of extracts (n = 3) of biofilms of *P. lipolytica* TC8 obtained with various phosphate concentrations (from 10^{-4} to 1.32 mM).

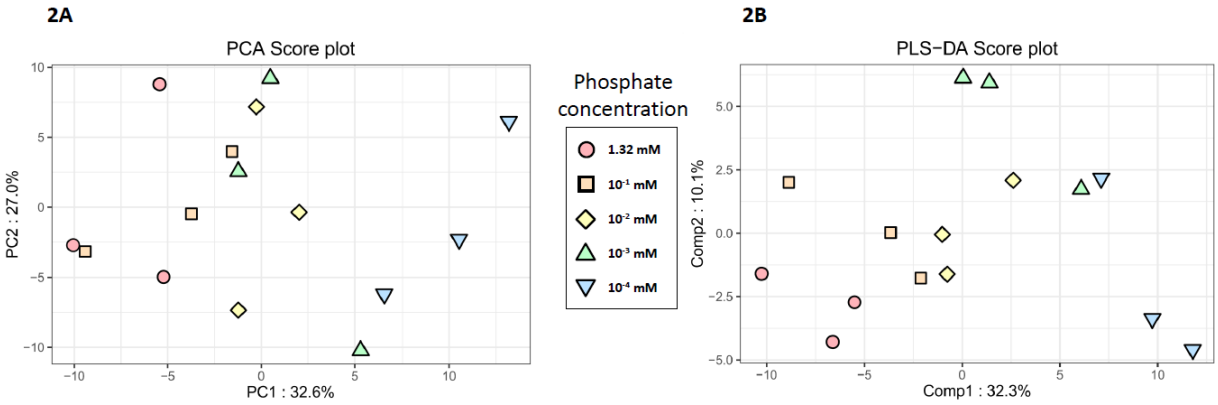

Figure 3. Molecular network built with (+)-ESI-LC-MS/MS data of extracts of biofilms of *P. lipolytica* TC8 with putatively annotated nodes and also MS/MS spectra and MS/MS fragmentation patterns of two specific compounds [PE (14:0/14:0) and OL (16:0/16:0)].

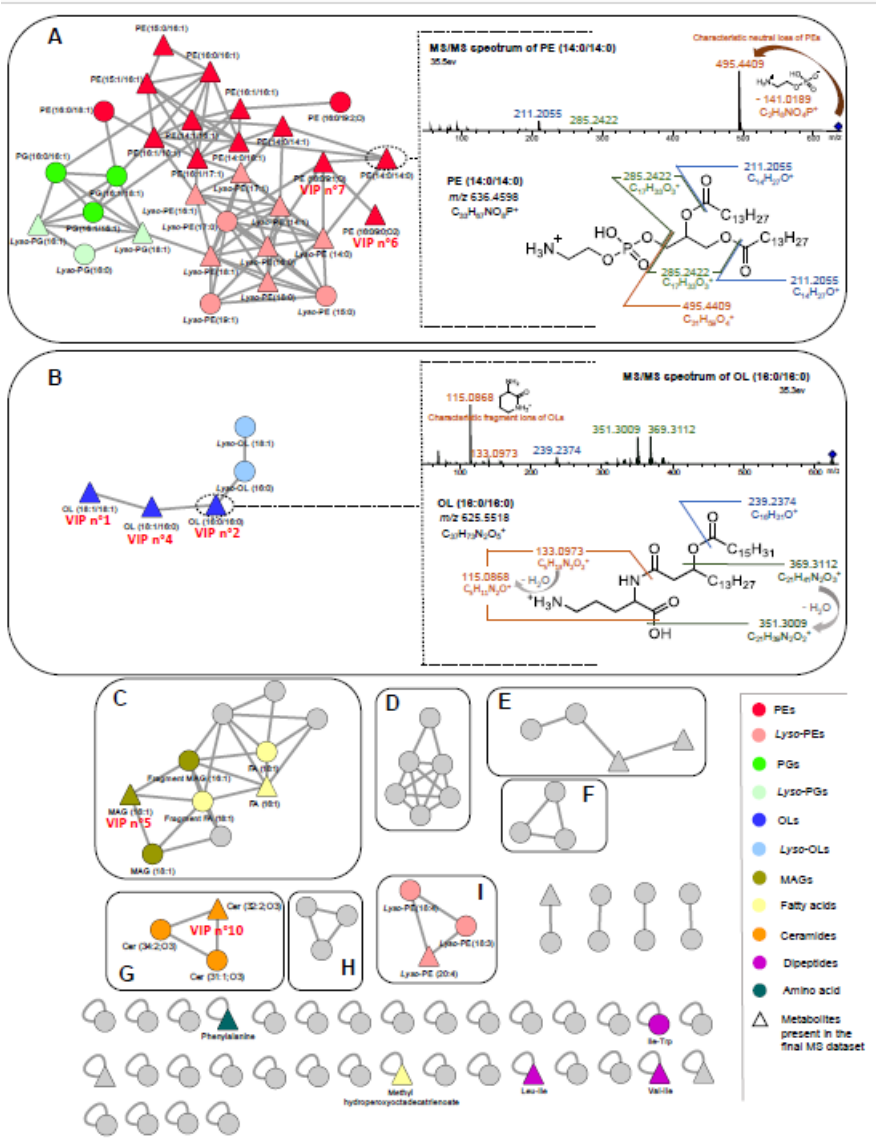

Figure 4. Normalized concentrations of the eight metabolites with the highest VIP scores implied in the chemical discrimination between biofilms of *P. lipolytica* TC8 grown with various phosphate concentrations (from 10^{-4} to 1.32 mM). *p*-values and "**a**," "**b**," "**c**" indexes corresponded to the results of one-way ANOVA analyses and post hoc tests (HSD Tukey's test), respectively.